RSC Advances

PAPER

View Article Online
View Journal | View Issue

Cite this: *RSC Adv.*, 2023, **13**, 11464

Enhanced inhibition of protein disulfide isomerase and anti-thrombotic activity of a rutin derivative: rutin:Zn complex†

Xinyuan Liao,[a] Panpan Ji,[b] Kunxiang Chi,[a] Xueying Chen,[a] Yang Zhou,[a] Shanli Chen,[a] Yuan Cheng,[a] Robert Flaumenhaft,[c] Cai Yuan*[b] and Mingdong Huang *[a]

Received 20th February 2023
Accepted 17th March 2023

DOI: 10.1039/d3ra01135f

rsc.li/rsc-advances

Rutin is a flavonoid that exists in plants and in commonly consumed foods. In recent years, rutin has been demonstrated to have anti-thrombotic efficacy through its inhibition of protein disulfide isomerase. However, the low aqueous solubility and high dose limit the therapeutic applications of rutin. In this study, we found that the chelation of zinc ions increased rutin aqueous solubility by 4-fold. More importantly, the thus-formed rutin:Zn complex inhibited PDI activity more potently than rutin itself. In a murine model with electric current-induced arterial thrombosis, the rutin:Zn complex slowed mouse arterial occlusion compared to rutin without increasing bleeding risk. Thus, the zinc chelation not only improved rutin aqueous solubility but achieved stronger inhibition of PDI. Furthermore, zinc chelation of a selected list of flavonoids containing the adjacent keto and phenoxy groups also increased their inhibition of PDI. Hence, our study provides a strategy to promote flavonoids' anti-thrombotic properties.

1. Introduction

Flavonoids are a class of natural substances commonly found in vegetables, grains, fruits, wine and tea. Flavonoids have been shown to have a range of biological activities, including anti-oxidative,[1] anti-inflammatory,[2] and anti-mutagenic[3,4] activities. In addition, flavonoids play a significant role in cardiovascular diseases.[5] Quercetin-3-*O*-rutinoside (rutin) is a member of the flavonoid family. In previous studies, rutin was identified as an anti-thrombotic molecule by inhibiting protein disulfide isomerase (PDI),[6] which is an endoplasmic reticulum (ER)-resident chaperone protein facilitating disulfide bond formation. PDI can also be released into the extracellular environment, and this pool of extracellular PDI was shown to play a critical role in thrombosis.[7] Recently, we identified the molecular binding site of rutin on PDI using both structural biology and mutagenesis techniques, and demonstrated that rutin occupies the major substrate binding site located at the b′ domain of PDI with residue H256 as the key residue.[8] Rutin was shown to significantly reduce thrombin generation in humans without inducing bleeding side effects.[6] Despite their wide biological functions, flavonoids have low bioavailability and low druggability, partly due to limited gastrointestinal absorption, rapid degradation and excretion, leading to low the requirement of a high dose to induce an anti-thrombotic effect in clinical trials.[9]

There are intensive research efforts to improve the bioavailability of rutin. For example, the Swiss company Zyma Pharma first described a synthesis of hydroxyethyl derivatives of rutin, named troxerutin, by reacting rutin with a hydroxyl ethylation agent. Troxerutin showed significantly enhanced rutins' bioactivity, including anti-oxidant, anti-inflammatory, anti-diabetic and anti-tumor.[10] However, numerous side effects (*e.g.* yellow discoloration of the skin, abnormal liver function) of troxerutin have been reported.[11] An alternative approach used nanoparticle systems to overcome the poor bioavailability. Recently, we developed a self-nano emulsifying drug delivery system of rutin (NanoR) to increase the solubility, and showed that orally administered NanoR prolonged the occlusion formation time.[12]

Metal ion chelation was also shown to improve rutin solubility, and also shown to enhance rutin's bioactivity.[13–15] Pan *et al.* developed a sodium rutin formulation (NaR). The NaR was showed to attenuate neuroinflammation and ameliorate synaptic plasticity impairment, reversing the deficits in spatial learning and memory in Alzheimer's animal models.[16] Zinc ions were shown to enhance flavonoids' bioactivity and likely bind to electron donor groups of flavonoids, including phenoxy and keto groups.[13,14] Selvaraj *et al.* prepared rutin:Zn complex and showed this rutin:Zn complex facilitated osteoblast differentiation *via* activating molecular signaling.[17] Zinc ion binding to rutin also enhanced the anti-oxidant capacity of rutin.[18]

[a]*College of Chemistry, Fuzhou University, Fujian 350108, China. E-mail: HMD_lab@fzu.edu.cn*

[b]*College of Biological Science and Engineering, Fuzhou University, Fuzhou, Fujian, 350108, China. E-mail: cyuan@fzu.edu.cn*

[c]*Division of Hemostasis and Thrombosis, Beth Israel Deaconess Medical Center, Harvard Medical School, Boston, MA 02215, USA*

† Electronic supplementary information (ESI) available. See DOI: https://doi.org/10.1039/d3ra01135f

In this study, we prepared a rutin:Zn complex by chelating rutin with zinc acetate, and showed that the complex has 1 : 2 stoichiometric ratio of rutin:Zn. Importantly, zinc ion chelation also improved the inhibitory effects of rutin on PDI *in vitro* and prolonged clot formation time *in vivo*. In addition, we measured the zinc ion binding of a list of flavonoid analogs bearing similarity to rutin, and showed that zinc chelation significantly increased these flavonoids' inhibition to PDI reductase activity. Thus, our study showed zinc ion chelation is likely a general strategy to improve the bioavailability and bioactivity of flavonoids. It is plausible that other metal ions, like ferric and copper, could also chelate flavonoids and enhance their beneficial effects. However, further studies are needed to demonstrate such application.

2. Materials and methods

2.1 Preparation of flavonoid:Zn complex

Flavonoid:Zn was prepared as previously described with slight modification.[14] The zinc acetate (100 mM, CAS:557-34-6, Macklin) and flavonoid molecules (10 mM, purchased from YuanYe Inc.) were dissolved with DMSO separately, and were mixed (in 10 : 1 molar ratio) together to a total volume of 2 mL for 10 min at the room temperature. The mixture was then poured into 20 mL methanol to generate precipitate, which was washed with methanol 3 times and dried at 37 °C to yield the flavonoids:Zn complex. The yield of the flavonoid–Zn complex was 50%.

The complex was characterized by a reverse phase chromatography (RPC) column on an FPLC instrument (AKTA™ Pure, GE Healthcare), which was pre-equilibrated with chromatography grade water containing 5% acetonitrile. The rutin:Zn complex was eluted with a gradient of 5% to 80% of acetonitrile at a flow rate of 1 mL min^{-1}. The key in this experiment was not to add any trifluoroacetic acid, which is commonly used on C18 column at 0.1% but can disrupt the complex in our case.

2.2 Characterization of rutin:Zn complex

For UV-vis and fluorescence spectra measurements, rutin or rutin:Zn complex was diluted in either DMSO or ddH_2O at room temperature. UV-vis spectra were recorded using a standard 1.00 cm quartz cell over the range of 250–600 nm. The fluorescence was measured using SpectraMax spectrophotometer with the excitation at 430 nm, and the emission at 460–650 nm.

The elemental analysis was carried out on vario MACRO cube, which gave %C 38.27, %H 5.19, and %N < 0.03. The Zn content (12.05%) was measured using inductively coupled plasma mass spectrometry (ICP-MS). These data were consistent with a molecular formula of rutin:$((Zn(OAc)_2)_2(H_2O)_6)$, which gave calculated contents of %C 38.73%, %H 5.01%, %N 0, and %Zn 13.27. Fourier transform infrared spectroscopy (FTIR) spectra were collected in a Spectrum 2000 FTIR spectrometer in KBr pellets over the range of 400–4000 cm^{-1}. The thermogravimetric analysis (TGA) was measured on STA449C/6/G, Jupiter. The mass of each sample was 5 mg. The carrier gas was nitrogen at a flow rate of 50 mL min^{-1}. The samples were heated from 25–800 °C, and the mass change was recorded.

2.3 Recombinant protein expression and purification

The expression and purification of the recombinant proteins were carried out as previously reported.[19] The recombinant strain was cultured in the 500 mL LB medium with 100 μg mL^{-1} ampicillin at 37 °C for 6 h. The IPTG (isopropyl-*β*-D-thiogalactoside) was added when the OD_{600} reached 0.6 for the induction of protein expression at 18 °C. After 12 h induction, the cells were harvested by centrifugation at 3000*g* for 20 min. The cell pellets were re-suspended at 40 mM Tris–HCl (pH 7.4), 150 mM NaCl, 5% glycerol (v/v), 1 mM DTT. The lysate was crushed at 600 Pa pressure and centrifuged at 12 000*g* for 40 min. The target protein was captured from the supernatant using affinity chromatography with Ni Sepharose™ excel resin (GE healthcare), and eluted with the elution buffer containing 40 mM Tris–HCl (pH 7.4), 150 mM NaCl, 5% glycerol (v/v), 1 mM DTT and 500 mM imidazole. The eluted protein was further purified by gel filtration chromatography using Superdex 200 HR 10/300 column (GE Healthcare), which was pre-equilibrated with the buffer containing 40 mM Tris–HCl (pH 7.4), 50 mM NaCl, 5% glycerol (V/V), 1 mM DTT. The purified protein was stored at −80 °C.

2.4 Fluorescence-based direct binding assay

Direct binding of rutin or rutin:Zn complex to PDI-b′x was measured based on the intrinsic fluorescence of rutin. Different doses of recombinant proteins were incubated with 50 μM rutin or rutin:Zn complex in a black 96-well plate at 25 °C for 30 min before measurements. The fluorescence emission spectrum of each well was measured with the excitation at 430 nm at room temperature on a BioTek Synergy microplate reader with a sensitivity of 100 or 120 and measurements of per data with 100 times.

2.5 Insulin turbidity assay

Rutin or rutin:Zn complex (50 μM) was added into 1.8 μM PDI and incubated together with 600 μM insulin, 1 mM DTT, 2 mM EDTA, pH 7.4, in a 96-well plate for 30 min at 37 °C, followed by the turbidity measurement at 650 nm on SpectraMax spectrophotometer. The total volume of wells was maintained at 100 μl, and the reaction was monitored for 1.5 h.

2.6 Thrombin generation assay

The whole blood from volunteers was centrifuged at 160 g for 20 min to isolate the platelet rich plasma (PRP). The PRP (30%) was incubated with 5 mM Gly-Pro-Arg-Pro peptide, 5 mM $CaCl_2$ and stimulated with 0.1 U mL^{-1} thrombin in the buffer containing 20 mM Tris (pH 7.4) and 150 mM NaCl, followed by the addition of 1.8 μM PDI. To compare the inhibition efficacy, rutin or rutin:Zn complex was added to 35 μM. The samples were then diluted at 1 : 4 ratio into PBS containing 80 μM chromogenic substrate S2288 and 12.5 mM EDTA. The reaction

was monitored at 25 °C by recording the absorbance at 405 nm on Spectra Max i3x spectrophotometer for 30 min.

2.7 Clot formation assay

The PRP (30%) and 1.8 μM PDI were incubated with different doses (35 and 50 μM) of rutin, or rutin:Zn complex, in a buffer containing 20 mM Tris (pH 7.4), and 150 mM NaCl at 37 °C for 20 min. Subsequently, 5 mM $CaCl_2$ (final concentration) was added to trigger the clot formation. The reaction was monitored by recording the absorbance at 405 nm for 30 min on a microplate reader (Spectra Max i3x, Molecular Devices, San Jose, CA).

2.8 Direct current-induced arterial thrombosis murine model

About 20 gram healthy male ICR mice (provided by Experimental Animal Center, Fuzhou) were randomly divided into 4 groups ($n = 6$), and injected with saline, rutin, or rutin:Zn complex (0.5 mg kg^{-1} or 1.0 mg kg^{-1} of body weight) *via* tail vein. After 10 min, the mice were anesthetized by 1.5% sodium pentobarbital (30 mg kg^{-1}), and the carotid was exposed. The current-induced probe (animal thrombus formation instrument YLS-14B, Ji'nan Yiyan Technology Development Co., Ltd, Ji'nan, China) was placed around the left common carotid artery. The artery was stimulated with 0.5 mA current, and the arterial flow was monitored until the artery was occluded (defined as no flow for ≥2 min). Finally, the times to occlusion the artery were recorded at the end of the assay. All animal experiments were carried out in accordance with the guidelines for the control and supervision of laboratory animals as approved by the institutional animal ethics committee at Fuzhou University.

2.9 Tail bleeding assay

The tail bleeding time was measured as previously described.[12] Basically, healthy male ICR mice (about 20 gram) were randomly infused by tail vein with the saline, 0.5 mg kg^{-1} rutin or rutin:Zn complex. After 10 min, the tail of the mice was cut at 0.5 cm from the tip, and immediately immersed into a 10 mL tube containing 8 mL of pre-warmed saline. The time when the bleeding stopped was recorded.

2.10 Statistics

All data represented the mean from triplicate measurements. Significance compared with the control is denoted by * for $p < 0.05$, ** for $p < 0.01$, or *** for $p < 0.001$.

3. Results

3.1 Preparation and characterization of rutin:Zn complex

We prepared rutin:Zn by adding zinc acetate solution into rutin (Fig. S1†) and precipitated the complexes with methanol.

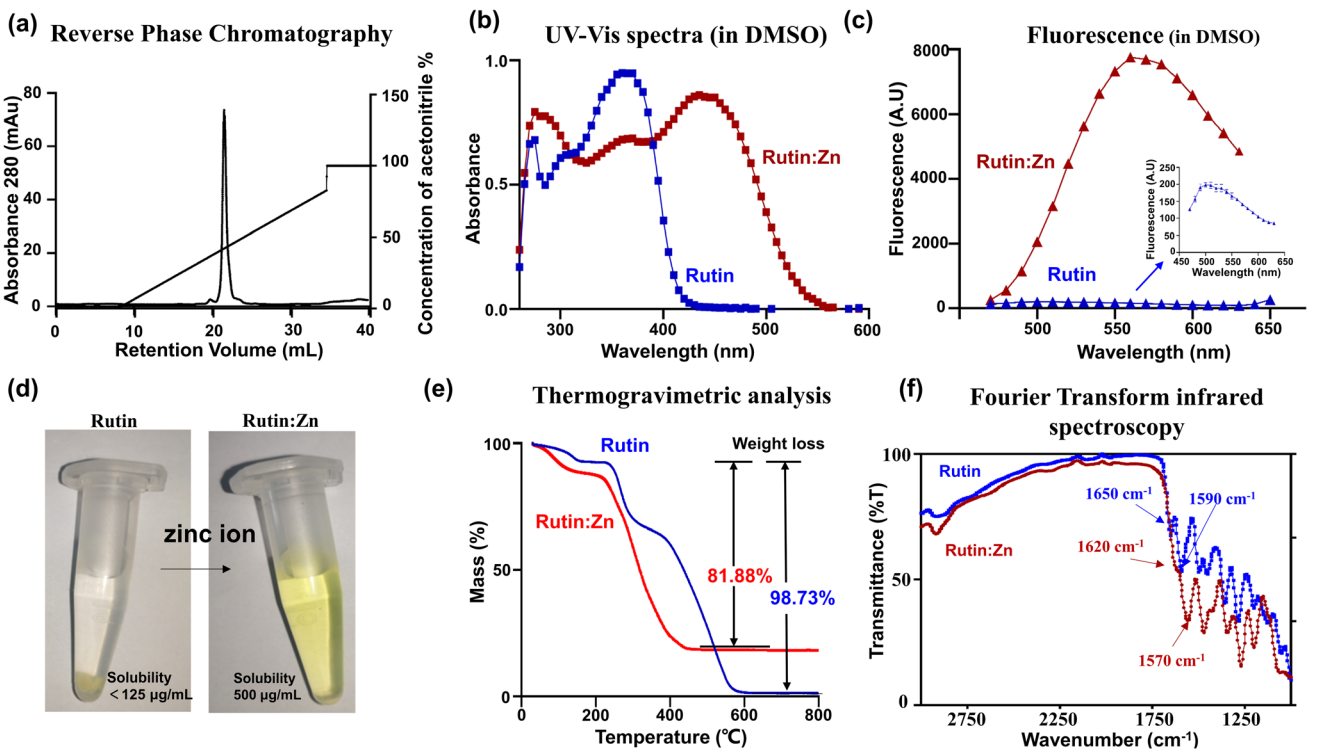

Fig. 1 Characterization of rutin:Zn complex. (a) Rutin:Zn complex is highly pure, as demonstrated by reverse phase chromatography. (b) Zinc chelation induced red-shift of the UV-vis spectra of rutin in DMSO. (c) Zinc chelation enhanced the fluorescence emission of rutin in DMSO. (d) Rutin:Zn (right) was dissolved to a higher concentration in water than rutin (left, with precipitation), indicating its significantly enhanced aqueous solubility. (e) Thermogravimetric analysis of rutin (blue) and rutin:Zn complex (red). The residual weight of the complex did not fall to zero at high temperature due to the presence of zinc, giving the ratio of rutin:Zn of about 1 : 2. (f) The transform infrared spectroscopy of rutin:Zn complex showed reduced C=O stretching vibration at the adjacent keto and phenoxy group than rutin.

The rutin:Zn complex was shown to have high homogeneity by reverse phase chromatography (Fig. 1a). The as-prepared complexes showed a red-shift in their UV-vis spectra in DMSO compared to the original flavonoids (Fig. 1b). On fluorescence emission spectrum, rutin:Zn showed significantly stronger fluorescence intensity than rutin itself (Fig. 1c), and its emission peak was slightly red-shifted (em 550 nm *vs.* ~530 nm). Importantly, the aqueous solubility of rutin:Zn complex was significantly increased compared to rutin by 4-fold (500 *vs.* 125 mg mL^{-1}, Fig. 1d). To study whether the rutin:Zn complex was stable in the aqueous solution, we measured the UV-vis spectra in H_2O of rutin:Zn complex and found a clear bathochromic shift of its maximal absorption compared with rutin (345 nm *vs.* 365 nm, Fig. S2a†). Meanwhile, the fluorescence of rutin:Zn complex was also stronger than rutin when dissolved in H_2O (Fig. S2b†), demonstrating the zinc ion did not dissociate after rutin:Zn complex dissolved in the H_2O.

Next, we used the inductively coupled plasma mass spectrometry (ICP-MS) data to measure the amount of zinc in the complex, which gave a high zinc content (13.7%), clearly demonstrating the a rutin:Zn ratio of 1 : 2. For comparison, a ratio of 1 : 1 would give a zinc content of 8.99%. Further elemental analysis on CHN gave a molecular formula of rutin:$(Zn(OAc)_2)_2(H_2O)_6$. In thermogravimetric (TGA) analysis, rutin almost completely burnt off at high temperatures (>600 °C, Fig. 1e), losing 98.73% of its weight. For comparison, the rutin:Zn complex lost only 81.88% (cal. 85.2% based on the formula of rutin:$((Zn(OAc)_2)_2(H_2O)_6)$ of its weight on thermogravimetric graph at a temperature higher than 450 °C (Fig. 1e). These results further supported the rutin:Zn ratio of 1 : 2.

The Fourier Transform Infrared (FTIR) measurement (Fig. 1f) displayed a shift of rutin carbonyl stretching vibration from 1650 to 1620 cm^{-1} upon zinc chelation, indicating direct interaction of zinc to the carbonyl group in position 4 of rutin. Thus, one Zn ion binds to the 4-keto,5-phenoxy group of rutin. Another zinc ion binds to other phenoxy groups, and most likely binds to and 3′,4′-phenoxy groups of the B ring due to the chelation effect. Such chemical structure of the rutin:Zn complex is shown in Fig. S3.†

3.2 Rutin:Zn showed stronger inhibition against PDI than rutin

Our recent work demonstrated that rutin directly inhibited protein disulfide isomerase (PDI) activity, leading to an antithrombotic effect.[6] Here, we compared the binding of rutin and rutin:Zn complex to PDI in a direct binding assay based on the change of intrinsic fluorescence of rutin. The inherent fluorescence of rutin has maximal emission around 530 nm. The addition of different concentrations of PDI increased the fluorescence intensity of rutin and caused a red shift of the maximal emission wavelength to about 550 nm, demonstrating the direct molecular interaction of rutin with PDI.[8] Our results showed that the presence of PDI in either rutin or rutin:Zn complex significantly increased the rutin's fluorescence in a dose-dependent manner (Fig. 2a), demonstrating the direct molecular interaction of PDI to rutin or rutin:Zn complex. The rutin:Zn showed a comparable PDI binding than rutin itself (Ki of 3.19 μM *vs.* 5.20 μM).

We also measured the effect of rutin:Zn complex on PDI reductase activity using insulin turbidity assay.[20] The disulfide bonds of insulin were reduced by PDI in the presence of DTT, leading to the cross linking of the insulin and the development of turbidity of insulin solution, which can be measured at 650 nm and is proportional to the PDI reductase activity. Our results showed rutin:Zn complex had a more potent inhibition of PDI reductase activity than rutin at the same concentration (Fig. 2b), demonstrating the zinc ion chelation increased rutin's inhibition of PDI.

3.3 Rutin:Zn inhibited thrombus formation stronger than rutin

PDI has recently been shown to participate in thrombus formation, and extracellular PDI is an alternative target of antithrombotic therapy.[6,21] To measure the potential antithrombotic effects of rutin:Zn complex, we first used a chromogenic assay to analyze thrombin generation in human blood (Fig. 3a). PDI has been shown to be involved in the initiation and burst of thrombin formation.[6,21] Indeed, the addition of exogenous recombinant PDI increased thrombin formation

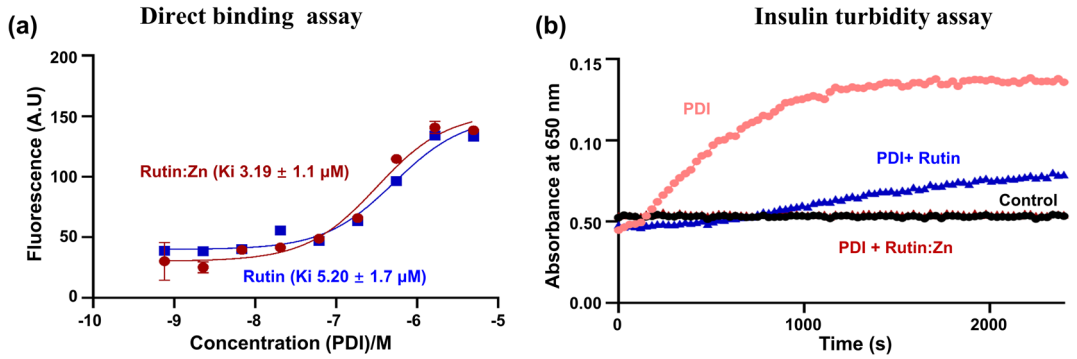

Fig. 2 Rutin:Zn showed slightly higher binding affinity and stronger inhibitory effects against PDI than rutin. (a) The intrinsic fluorescence of rutin or rutin:Zn complex increased in the presence of an increasing concentration of PDI-b′x protein, giving a binding Ki of 3.19 μM for the complex and 5.2 μM for rutin. (b) Rutin:Zn inhibited PDI activity more potently than rutin in insulin reductase assay.

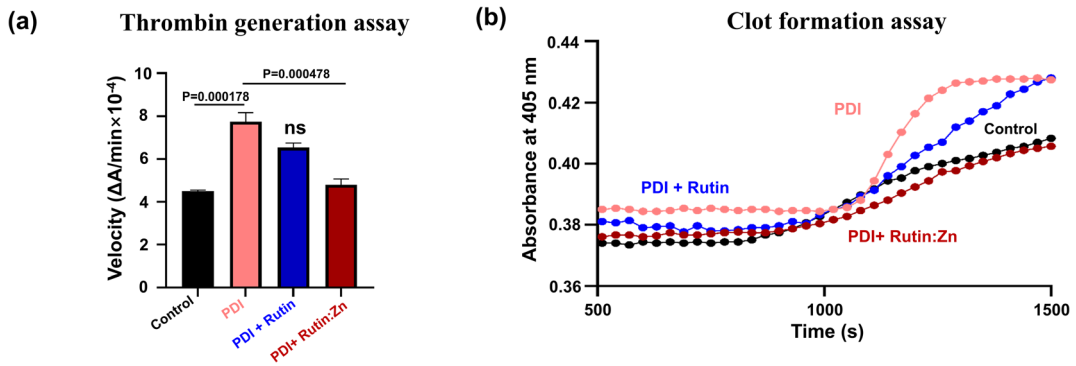

Fig. 3 Rutin:Zn showed stronger inhibitory effects in PDI-triggered thrombus formation than rutin *in vitro*. (a) Rutin:Zn displayed stronger inhibition on thrombin generation assay than rutin (both at 35 μM). (b) Rutin:Zn (35 μM in DMSO) showed significant inhibition in clot formation assay, leading to lower clot formation. Values represented the mean ± SE of triplicate experiments. Significance compared with the control is denoted by $*p < 0.05$,$**p < 0.01$,$***p < 0.001$.

(Fig. 3a). Rutin:Zn treatment significantly reduced thrombin formation compared with rutin treatment group. These results further indicated rutin:Zn complex exhibited greater inhibitory efficacy than rutin in anti-thrombotic application.

To further validate this result, we evaluated the anti-coagulation function of rutin:Zn complex in the plasma sample using a kinetic clot formation assay on microplates, where the clot formation was triggered using 10 mM calcium ion. The results showed that PDI enhanced clot formation, and such enhancement was reduced by incubation with rutin:Zn or rutin in 35 μM (Fig. 3b). Notably, rutin:Zn, but not rutin, inhibited clot formation to the baseline level. These results clearly demonstrated that rutin:Zn had a stronger capacity to inhibit PDI than rutin, consistent with the results of the insulin turbidity assay.

3.4 Rutin:Zn complex significantly prolonged artery occlusion time in current-induced arterial thrombosis without prolonging bleeding

Rutin was previously shown to have an anti-thrombotic effect in mice without prolonging bleeding.[6,20] We evaluated the effect of zinc ion on rutin's anti-thrombotic activity *in vivo* using a direct current-induced arterial thrombosis murine model (Fig. 4a). This model uses electric current (0.5 mA) to directly injure the endothelium of the common carotid artery of mice, inducing thrombus formation and completely occlusion the artery. The artery occlusion time in the control group was 154 ± 37 s. At a dose of 0.5 mg kg^{-1} of body weight, the artery occlusion time was prolonged to 234 ± 28 s in the rutin-treated group, and the time was further extended to 435 ± 65 s in the rutin:Zn complex-treated group, which was 2.8-fold compared to the control

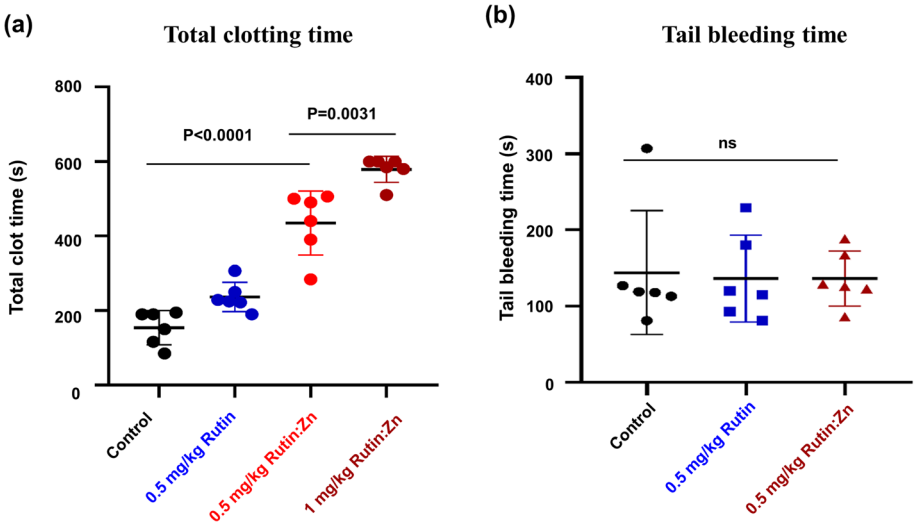

Fig. 4 Rutin:Zn reduced blood occlusion formation in mice compared to rutin and did not affect blood hemostasis based on tail bleeding time. (a) Rutin:Zn significantly prolonged the occlusion time of mouse carotid artery in mouse thrombosis model. (b) The tail bleeding time of rutin:Zn was comparable to rutin and the control. Values represented the mean ± SE of triplicate experiments. Significance compared with the control is denoted by $*p < 0.05$, $**p < 0.01$, $***p < 0.001$.

group and 1.8-fold compared to the rutin-treated group. A higher dose of rutin:Zn complex (1 mg kg^{-1} of body weight) further prolonged the occlusion time to 579 ± 23 s. Together, these results demonstrate the powerful anti-thrombotic effect of rutin:Zn complex.

Next, we measured the effect of rutin:Zn complex on hemostasis using the mouse tail bleeding assay as we previously described (Fig. 4b).[12] The bleeding time of the control group mice was 144 ± 81 s. Importantly, rutin:Zn complex at 0.5 mg kg^{-1} of body weight showed a comparable bleeding time (136 ± 36 s) to the saline group (144 ± 81 s) and the rutin group (136 ± 57 s). These results indicated that rutin:Zn complex did not compromise normal blood hemostasis.

3.5 Zinc chelation to adjacent keto and phenoxy groups enhanced flavonoid inhibition of PDI reductase activity

We further investigated the effect of zinc ion using four additional flavonoids (kaempferol, quercetin, isoquercitrin, and (−)-epicatechin) that are commercially available and structurally similar to rutin (Fig. 5). These flavonoids themselves showed limited inhibition on PDI reductase activity in the insulin turbidity assay (Fig. 5). Upon the addition of zinc ions, kaempferol, quercetin, and isoquercitrin showed stronger inhibition on PDI reductase activity (Fig. 5a–c). In contrast, (−)-epicatechin:Zn complex did not inhibit PDI activity at all, similar to epicatechin itself (Fig. 5d). The first three compounds contain the 4-keto,5-phenoxy moiety, while (−)-epicatechin contains 3′,4′-catechol moiety but not 4-keto,5-phenoxy moiety. Thus, these results demonstrated the importance of chelating Zn^{2+} to the adjacent keto and phenoxy group of flavonoids for enhancing their inhibitory efficacy against PDI.

It should be mentioned that the addition of zinc ion perturbed the UV-vis spectra of the flavonoids with 4-keto,5-phenoxy moiety (the first three flavonoids, Fig. S4a–c†), but not (−)-epicatechin (Fig. S4d†), demonstrating that this moiety, but not catechol, is the primary binding site for zinc ion, consistent with previous studies that showed 1,2-dihydroxybenzene has a weak chelating affinity to zinc ion.[22]

4. Discussion

A range of different metal ions are reported to bind to flavonoids, including Na^{+}, Zn^{2+}, Cu^{2+}, Fe^{3+}, and others.[14,23,24] Both Cu^{2+} and Fe^{3+} ions can function as oxidants and can oxidize amino acids,[25] *e.g.*, methionine and cysteine. In addition, these two ions can be catalysts for the Fenton reaction, which activates molecular oxygen and generates reactive oxygen species. Due to these properties, Cu^{2+} and Fe^{3+} ions can damage proteins and even flavonoids. In contrast, zinc ions are not redox-active metal ion, and thus will likely be more amenable in biological applications.

Zinc ions likely bind to electron donor groups of flavonoids, including phenoxy and keto groups. As a flavonoid, rutin contained a total of 10 hydroxyl groups, with two attached to the A ring (positions 5 and 7), two at the B ring (positions 3′ and 4′), and six distributed on the glucopyranosyl (positions 2″, 3″, and 4″) and rhamnopyranosyl (positions 2‴, 3‴, and 4‴) units. The catechol group at the B ring (positions 3′ and 4′), and also the keto and phenoxy group at the C4, C5 positions of ring C, are two more probable binding sites for zinc ions due to the chelating effect where one zinc ion binds to two oxygen atoms. In a 2014 independent synthesis of rutin:Zn complex, the authors prepared the complex by titrating different concentrations of zinc chloride (1 : 4, 1 : 2) into the 5 mM solutions of rutin in mixed solvents of DMSO/Tris (pH 7.2),[26] and showed the zinc ion chelation to rutin in either 1 : 1 ratio (with zinc binding to A-C rings), 1 : 2 (with zinc binding to A-C-B rings) or 2 : 1 ratio (with zinc binding to A-C rings) based on proton NMR and mass spectrometry studies. A different study by Ikeda *et al.* also reported that zinc ion chelated to rutin at 1 : 2 ratio with zinc binding to 4-keto,5-phenoxy positions (A-C ring) and 3′,4′-position catechol moiety (B ring). This different zinc chelation mode was again confirmed in a recent independent study by Harold *et al.*[27] Moreover, Harold *et al.* also observed differential rutin:Zn stoichiometric ratios in DMSO (1 : 2, with zinc binding to A-C-B rings) and methanol solution (2 : 1, with zinc binding to A-C rings).[27] Here, we prepared the rutin:Zn complex similar to

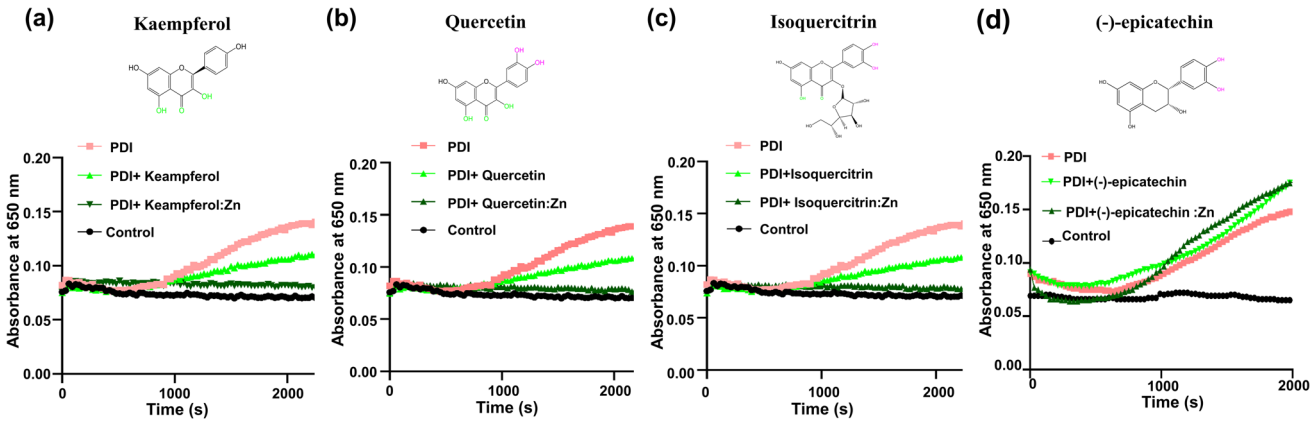

Fig. 5 The adjacent keto and phenoxy groups are critical for chelating zinc ions to increase the inhibitory effect of rutin against PDI in insulin turbidity assay. The presence of zinc ions significantly increased kaempferol (a); quercetin (b); isoquercitrin (c) inhibitory effect against PDI reductase activity compared to native flavonoids, while (d) (−)-epicatechin:Zn showed no inhibitory efficacy against PDI.

Ikeda *et al.* paper but with some modifications. Our results showed zinc ions bind to rutin at the 4-keto,5-phenoxy positions and the 3′,4′-catechol moiety positions in a 1 : 2 ratio.

Recently, we delineated the direct molecular interaction of PDI with rutin and employed NMR spectroscopy, mutagenesis, function assay, and molecular dynamics to show that PDI residue H256 is the key mediating the interaction between PDI and rutin, and the analogs without a phenoxy group at 7-position showed no binding to PDI, which demonstrated an essential role of the 7-position phenoxy group for binding to PDI.[8] Moreover, the flavonoid analogs without a phenoxy group at the 7-position showed no binding to PDI, which demonstrated an essential role of the 7-position phenoxy group for binding to PDI. In this study, we did not choose a sodium rutin formulation (NaR), because the sodium of NaR chelates at the 7-position of rutin,[16] which may intervene with rutin interaction with PDI. Here, we found that the rutin:Zn maintained the direct interaction to PDI. In addition, we found that mutant H256 of PDI also abolished rutin:Zn inhibition efficacy to PDI reductase activity (Fig. S5†), demonstrating that zinc ion chelation did not affect the rutin 7-position phenoxy group binding to PDI.

In this work, rutin:Zn complex appeared to be more effective in blocking PDI-triggered thrombotic events compared to rutin itself. In addition, our structure-functional activity study of four additional flavonoids further supported the adjacent keto and phenoxy group were critical for increasing flavonoid:Zn complexes inhibition of PDI. Upon zinc ion chelation, the flavonoids containing the adjacent keto and phenoxy group exhibited a significant increase in inhibition of PDI (*e.g.* quercetin, isoquercitrin). The inhibition enhancement also happened in the compounds containing only the adjacent keto and phenoxy moiety (*e.g.* kaempferol). Based on the structure of rutin:Zn, we generated the molecular dynamic model of its interaction with PDI (Fig. S6a†). This model reveals that the zinc chelated at rutin's 4-keto,5-phenoxy, which was then embedded in the major binding pocket on the b′ domain and prevented other substrates from binding to PDI. In contrast, the 3′-,4′-catechol moiety of rutin was located at the periphery of the substrate binding site and was solvent exposed, thus its interaction with PDI may be weak and transient, and zinc ion chelation with the catechol group would not affect rutin binding to PDI. Our results of the structure-functional activity study further supported this model. Moreover, we also developed a probe-based assay using a molecular substrate smaller than insulin.[8] Our results showed that adding either rutin:Zn complex or rutin inhibited PDI cleavage for the GSSG probe at comparable levels (Fig. S6b†). Such stronger inhibitory efficacy of the complex in the insulin reductase activity assay (Fig. 2b) but not in the GSSG cleavage assay was due to the difference in the substrate used in the assays. The insulin assay requires the insulin substrate to bind to the major substrate binding site at the b′ domain, while the GSSG probe is a dipeptide, much smaller than insulin, and interacted only with the catalytic sites of PDI in the a and a′ domain, but not with the major substrate binding located at the b′ domain.

In summary, this study showed the chelation of zinc to adjacent keto and phenoxy position was critical for enhancing rutin and flavonoids' inhibition to PDI, which provides a new strategy for the clinical translation of flavonoids.

Abbreviations

PDI	Protein disulfide isomerase
Rutin	Querctin-3-*O*-rutinoside

Author contributions

Xinyuan Liao: investigation, data curation, writing – original draft, visualization; Panpan Ji, Kunxiang Chi, Xueying Chen: resources, investigation; Zhou Yang, Shanli Chen, Yuan Cheng: investigation; Robert Flaumenhaft, Cai Yuan, Mingdong Huang: supervision, writing – review & editing, funding acquisition.

Conflicts of interest

There are no conflicts to declare.

Acknowledgements

This work is financially supported by grants from National Key R&D Program of China (2017YFE0103200), National Natural Science Foundation of China (22077016), Fujian Health and Education Ministry Joint Program (2019-WJ-17), and the Fujian Provincial Natural Science Foundation Projects (2021Y4008, 2022J02017 and 2019J06007).

References

1 J. Kang, Z. Li, T. Wu, G. S. Jensen, A. G. Schauss and X. Wu, *Food Chem.*, 2010, **122**, 610–617.
2 M. Serafini, I. Peluso and A. Raguzzini, *Proc. Nutr. Soc.*, 2010, **69**, 273–278.
3 M. Miyazawa and M. Hisama, *Biosci., Biotechnol., Biochem.*, 2003, **67**, 2091–2099.
4 K.-Y. Park, G.-O. Jung, K.-T. Lee, J. Choi, M.-Y. Choi, G.-T. Kim, H.-J. Jung and H.-J. Park, *J. Ethnopharmacol.*, 2004, **90**, 73–79.
5 M. Gross, *Pharm. Biol.*, 2004, **42**, 21–35.
6 R. Jasuja, F. H. Passam, D. R. Kennedy, S. H. Kim, L. van Hessem, L. Lin, S. R. Bowley, S. S. Joshi, J. R. Dilks, B. Furie, B. C. Furie and R. Flaumenhaft, *J. Clin. Invest.*, 2012, **122**, 2104–2113.
7 R. Flaumenhaft, *Curr. Opin. Hematol.*, 2017, **24**, 439–445.
8 X. Liao, X. Zhuang, C. Liang, J. Li, R. Flaumenhaft, C. Yuan and M. Huang, *J. Agric. Food Chem.*, 2022, **70**, 4475–4483.
9 B. Gullón, T. A. Lú-Chau, M. T. Moreira, J. M. Lema and G. Eibes, *Trends Food Sci. Technol.*, 2017, **67**, 220–235.
10 Z. Ahmadi, R. Mohammadinejad, S. Roomiani, E. G. Afshar and M. Ashrafizadeh, *J. Pharmacopuncture*, 2021, **24**, 1–13.

11 *Meyler's Side Effects of Drugs*, ed. J. K. Aronson, Elsevier, Oxford, 6th edn, 2016, p. 219.
12 D. Chen, Y. Liu, P. Liu, Y. Zhou, L. Jiang, C. Yuan and M. Huang, *Drug Delivery*, 2022, **29**, 1824–1835.
13 I. B. Afanas'eva, E. A. Ostrakhovitch, E. V. Mikhal'chik, G. A. Ibragimova and L. G. Korkina, *Biochem. Pharmacol.*, 2001, **61**, 677–684.
14 N. Andrades, E. Novak, D. Maria, A. Velosa and R. M. Pereira, *Chem. Biol. Interact.*, 2015, **239**, 184–191.
15 B. Gullón, T. Lú-Chau, M. T. Moreira, J. M. Lema and G. Eibes, *Trends Food Sci. Technol.*, 2017, **67**, 220–235.
16 R. Y. Pan, J. Ma, X. X. Kong, X. F. Wang, S. S. Li, X. L. Qi, Y. H. Yan, J. Cheng, Q. Liu, W. Jin, C. H. Tan and Z. Yuan, *Sci. Adv.*, 2019, **5**, eaau6328.
17 S. Vimalraj, S. Saravanan and R. Subramanian, *Chem.-Biol. Interact.*, 2021, **349**, 109674.
18 M. Bratu, *Rev. Chim.*, 2014, **65**, 544–549.
19 J. D. Stopa, D. Neuberg, M. Puligandla, B. Furie, R. Flaumenhaft and J. I. Zwicker, *JCI Insight*, 2017, **2**, e89373.
20 L. Lin, S. Gopal, A. Sharda, F. H. Passam, S. R. Bowley, J. D. Stopa, G. Xue, C. Yuan, B. C. Furie, R. Flaumenhaft, M. Huang and B. Furie, *J. Biol. Chem.*, 2015, **290**, 23543–23552.
21 J. Cho, B. C. Furie, S. R. Coughlin and B. Furie, *J. Clin. Invest.*, 2008, **118**, 1123–1131.
22 M. Sancho, S. Blanco, F. Ferretti, A. Jubert and E. Castro, *J. Argent. Chem. Soc.*, 2006, **943**, 143–155.
23 Y. Bai, F. Song, M. Chen, J. Xing, Z. Liu and S. Liu, *Anal. Sci.*, 2004, **20**, 1147–1151.
24 N. E. A. Ikeda, E. M. Novak, D. A. Maria, A. S. Velosa and R. M. S. Pereira, *Chem.-Biol. Interact.*, 2015, **239**, 184–191.
25 E. R. Stadtman and B. S. Berlett, *J. Biol. Chem.*, 1991, **266**, 17201–17211.
26 Y. Wei and M. Guo, *Biol. Trace Elem. Res.*, 2014, **161**, 223–230.
27 H. C. Da Silva, L. A. De Souza, H. F. Dos Santos and W. B. De Almeida, *ACS Omega*, 2020, **5**, 3030–3042.